

Titanium(IV) Citrate Speciation and Structure under Environmentally and Biologically Relevant Conditions

Joseph M. Collins, Ritika Uppal, Christopher D. Incarvito, and Ann M. Valentine*

Department of Chemistry, Yale University, P.O. Box 208107,
New Haven, Connecticut 06520-8107

Received December 30, 2004

The water-soluble complexes of Ti(IV) with citrate are of interest in environmental, biological, and materials chemistry. The aqueous solution speciation is revealed by spectropotentiometric titration. From pH 3–8, given at least three equivalents of ligand, 3:1 citrate/titanium complexes predominate in solution with successive deprotonation of dangling carboxylates as the pH increases. In this range and under these conditions, hydroxo- or oxo-metal species are not supported by the data. At ligand/metal ratios between 1:1 and 3:1, the data are difficult to fit, and are consistent with the formation of such hydroxo- or oxo- species. Stability constants for observed species are tabulated, featuring log β -values of 9.18 for the 1:1 complex $[\text{Ti}(\text{Hcit})]^+$, and 16.99, 20.41, 16.11, and 4.07 for the 3:1 complexes $[\text{Ti}(\text{H}_2\text{cit})_3]^{2-}$, $[\text{Ti}(\text{H}_2\text{cit})(\text{Hcit})_2]^{4-}$, $[\text{Ti}(\text{Hcit})_2(\text{cit})]^{6-}$, and $[\text{Ti}(\text{cit})_3]^{8-}$, respectively (citric acid = H_4cit). Optical spectra for the species are reported. The complexes exhibit similar yet distinct spectra, featuring putative citrate-to-Ti(IV) charge-transfer absorptions ($\lambda_{\text{max}} \approx 250\text{--}310\text{ nm}$ with $\epsilon \approx 5000\text{--}7000\text{ M}^{-1}\text{ cm}^{-1}$). The prevailing 3:1 citrate/titanium ratio in solution is supported by electrospray mass spectrometry data. The X-ray crystal structure of a fully deprotonated tris-citrate complex $\text{Na}_8[\text{Ti}(\text{C}_6\text{H}_4\text{O}_7)_3] \cdot 17\text{H}_2\text{O}$ (**1**) (or $\text{Na}_8[\text{Ti}(\text{cit})_3] \cdot 17\text{H}_2\text{O}$) that crystallizes from aqueous solution at pH 7–8 is reported. Compound **1** crystallizes in the triclinic space group $P\bar{1}$, with $a = 11.634(2)\text{ \AA}$, $b = 13.223(3)\text{ \AA}$, $c = 13.291(3)\text{ \AA}$, $V = 1982.9(7)\text{ \AA}^3$, and $Z = 2$.

Introduction

Titanium is the ninth most abundant element on Earth and the second most abundant transition metal, yet it is often thought to be inert in biology and the environment. Its coordination complexes, most commonly with the metal in the +4 oxidation state, feature a hydrolysis-prone Lewis acidic metal that quite easily forms oxide precipitates from aqueous solution.¹ Some coordination complexes of titanium(IV), however, are relatively stable to hydrolysis in aqueous solutions near neutral pH. Titanium(IV)–tris-catecholate complexes have been reported, for instance, that are hydrolytically stable up to pH 13.² The aqueous citrate complexes of titanium(IV), the focus of this investigation, are another such group.

Citrate complexes occupy a significant place in the materials, environmental, and medicinal chemistry of tita-

nium. Titanium(IV) citrate can serve as a soluble precursor to titanium oxide materials,³ for example, via the Pechini process. Conversely, moving from solid to solution, citrate and other organic α -hydroxy acids accelerate the dissolution of titanium from inert materials, including titanium oxide minerals in the environment⁴ and titanium metal in biomedical implants.⁵ The latter is relevant because citrate is one of the most important low-molecular-mass metal chelators in cellular fluids, having a concentration of approximately 0.1 mM in human plasma.⁶

In addition, some titanium compounds, including the citrate, are bioactive. Titanium(IV) citrate damaged and ruptured red blood cells through interactions with the cell membrane.⁷ Research into the anticancer activity of titanium

* Author to whom correspondence should be addressed. E-mail: ann.valentine@yale.edu. Tel: 203-432-5162.

- (1) Valentine, A. M. In *Encyclopedia of Inorganic Chemistry*; King, R. B., Ed.; John Wiley and Sons: Chichester, 2004.
- (2) Borgias, B. A.; Cooper, S. R.; Koh, Y. B.; Raymond, K. N. *Inorg. Chem.* **1984**, *23*, 1009–1016.

- (3) Cushing, B. L.; Kolesnichenko, V. L.; O'Connor, C. J. *Chem. Rev.* **2004**, *104*, 3893–3946.
- (4) Correns, C. W. In *Handbook of Geochemistry*; Wedepohl, K. H., Ed.; Springer: Berlin, 1969–1978; Vol. 2.
- (5) Strietzel, R.; Hosch, A.; Kalbfleisch, H.; Buch, D. *Biomaterials* **1998**, *19*, 1495–1499.
- (6) Martin, R. B. *J. Inorg. Biochem.* **1986**, *28*, 181–187.
- (7) Suwalsky, M.; Villena, F.; Norris, B.; Soto, M. A.; Sotomayor, C. P.; Messori, L.; Zatta, P. *J. Inorg. Biochem.* **2005**, *99*, 764–770.

compounds identified the serum protein transferrin as a potential titanium trafficking agent. Titanium(IV) citrate delivered titanium to that protein *in vitro*, producing the first reported titanium metalloprotein.^{8,9} Titanium(IV) citrate has been tested against tumors in rats.^{10,11} In that work, rats with Jensen's sarcoma were divided into two groups, one of which was treated with injections of Ti(IV) citrate. Three-week survival rates were 88% for the titanium-treated group, and 39% for the control group. Like some other soluble titanium compounds, Ti(IV) citrate exerts effects on the growth of plants.¹² Finally, Ti(III) citrate is produced *in situ* and used as a reductant for redox-active proteins and in cell culture.^{13,14} The byproduct of this reduction, presumably a Ti(IV) citrate species, remains in the solution or culture.

With its hard ligands, potential for chelation with multiple carboxylates, and ability to coordinate with its central bidentate α -hydroxy acid moiety to make a very stable 5-membered chelate, citrate is a good ligand for many intermediate to hard metals. In addition to complexes of higher nuclearity, several mononuclear metal complexes with citrate have been crystallographically characterized. The mononuclear complexes typically feature coordination of the metal to two citrate ligands through the α -hydroxy acid and one β -carboxylate, while the other β -carboxylate on each citrate dangles. Complexes of this type have been crystallized from aqueous solution near neutral pH for Mn(II) and Mn(III),¹⁵ Fe(III),¹⁶ Co(II),¹⁷ Ni(II),¹⁸ Cu(II),¹⁹ Zn(II),²⁰ Al(III), and Ga(III).²¹

Several important Ti(IV) citrate complexes were characterized recently, including an oxo-titanium complex with a Ti₈O₁₀ structural core.²² Tetranuclear²³ and dinuclear²⁴ com-

plexes of titanium with both peroxo and citrate ligands have been prepared. Dinuclear titanium complexes having only citrate ligands include (NH₄)₅[Fe(H₂O)₆][Ti(H₂cit)₃(Hcit)₃Ti] (from solution at pH 2.5–3.5) and Ba₃(NH₄)₇[Ti(cit)₃H₃(cit)₃-Ti] (from solution at pH 5–6).²⁵ In this paper, to reflect the ability of the citrate ligand to lose as many as four protons, the fully protonated citric acid (C₆H₈O₇) is designated H₄-cit, and thus, the citrate ligand with all three carboxylates as well as the hydroxyl deprotonated is designated cit.

Several mononuclear Ti(IV) complexes having only citrate ligands have been prepared and isolated from acidic aqueous solutions. Complexes of [Ti(H₂cit)₃]²⁻ with several different counterions crystallized at pH 1–2.8,^{25,26} and a complex of [Ti(H₂cit)(Hcit)₂]⁴⁻ crystallized at pH 2.8–4.²⁵ In each of these complexes, the metal coordinates three citrate ligands through the α -hydroxy acid moiety, leaving a total of six dangling carboxylates, all of which are protonated in the former complexes, and two of which are deprotonated in the latter. The characterization of these compounds represents important progress toward a full description of the aqueous coordination chemistry of Ti(IV) with citrate. The data also raise additional questions, including the following: What species are formed in solution under a range of conditions? What are the stability constants characterizing these species? What, if any, Ti(IV) citrate complexes are stable at neutral pH in aqueous solution? Do 3:1 citrate/Ti complexes also predominate in solution, or do 2:1 complexes (as seen for other first row transition metals) form, particularly as the remaining dangling carboxylates are deprotonated? Are dinuclear or higher complexes implicated?

Stability constants (β -values) and speciation for metal complexes in aqueous solution are classically determined by potentiometric titration.^{27–29} In cases where complexes formed have different UV/vis spectra, this technique can be combined advantageously with spectroscopic characterization of species. These data for Ti(IV) citrate have not yet been reported, likely because of the difficulties with titanium oxide precipitation if care is not taken to prevent this reaction. However, the β -values are important to have in hand as the contributions of titanium and titanium citrate compounds to materials, biological, environmental, and medicinal chemistry are studied. A previous study aimed to determine the stability constant of a titanium(IV) complex with citrate at pH < 1.3 by a different method, and attempted to reconcile these data with earlier work, also at low pH.³⁰ Notably, those results provided evidence against the formation of a di-ligand complex. Stability constants for citrates with titanyl species have been determined, again at low pH,³¹ although the importance of the titanyl species has been challenged.^{32,33}

- (8) Sun, H. Z.; Lin, H.; Weir, R. A.; Sadler, P. J. *Angew. Chem., Int. Ed. Engl.* **1998**, *37*, 1577–1579.
- (9) Guo, M. L.; Sun, H. Z.; McArdle, H. J.; Gambling, L.; Sadler, P. J. *Biochemistry* **2000**, *39*, 10023–10033.
- (10) Abragam, D. C. R. *Heb. Seances Acad. Sci.* **1935**, *200*, 990–991.
- (11) Schwietert, C. W.; McCue, J. P. *Coord. Chem. Rev.* **1999**, *184*, 67–89.
- (12) Kuzel, S.; Hruby, M.; Cigler, P.; Tlustos, P.; Van, P. N. *Biol. Trace Elem. Res.* **2003**, *91*, 179–190.
- (13) Zehnder, A. J. B.; Wuhmann, K. *Science* **1976**, *194*, 1165–1166.
- (14) Seefeldt, L. C.; Ensign, S. A. *Anal. Biochem.* **1994**, *221*, 379–386.
- (15) Matzapetakis, M.; Karlignano, N.; Bino, A.; Dakanali, M.; Raptopoulou, C. P.; Tangoulis, V.; Terzis, A.; Giapintzakis, J.; Salifoglou, A. *Inorg. Chem.* **2000**, *39*, 4044–4051.
- (16) Matzapetakis, M.; Raptopoulou, C. P.; Tsohos, A.; Papaefthymiou, V.; Moon, N.; Salifoglou, A. *J. Am. Chem. Soc.* **1998**, *120*, 13266–13267.
- (17) Matzapetakis, M.; Dakanali, M.; Raptopoulou, C. P.; Tangoulis, V.; Terzis, A.; Moon, N.; Giapintzakis, J.; Salifoglou, A. *J. Biol. Inorg. Chem.* **2000**, *5*, 469–474.
- (18) Zhou, Z. H.; Lin, Y. J.; Zhang, H. B.; Lin, G. D.; Tsai, K. R. *J. Coord. Chem.* **1997**, *42*, 131–141.
- (19) Bott, R. C.; Sagatys, D. S.; Lynch, D. E.; Smith, G.; Kennard, C. H. L.; Mak, T. C. W. *Aust. J. Chem.* **1991**, *44*, 1495–1498.
- (20) Swanson, R.; Ilsley, W. H.; Stanislawski, A. G. *J. Inorg. Biochem.* **1983**, *18*, 187–194.
- (21) Matzapetakis, M.; Kourgiantakis, M.; Dakanali, M.; Raptopoulou, C. P.; Terzis, A.; Lakatos, A.; Kiss, T.; Banyai, I.; Iordanidis, L.; Mavroumoustakos, T.; Salifoglou, A. *Inorg. Chem.* **2001**, *40*, 1734–1744.
- (22) Kemmitt, T.; Al-Salim, N. I.; Gainsford, G. J.; Bubendorfer, A.; Waterland, M. *Inorg. Chem.* **2004**, *43*, 6300–6306.
- (23) Kakihana, M.; Tada, M.; Shiro, M.; Petrykin, V.; Osada, M.; Nakamura, Y. *Inorg. Chem.* **2001**, *40*, 891–894.
- (24) Dakanali, M.; Kefalas, E. T.; Raptopoulou, C. P.; Terzis, A.; Voyiatzis, G.; Kyrikou, I.; Mavroumoustakos, T.; Salifoglou, A. *Inorg. Chem.* **2003**, *42*, 4632–4639.

- (25) Deng, Y. F.; Zhou, Z. H.; Wan, H. L. *Inorg. Chem.* **2004**, *43*, 6266–6273.
- (26) Zhou, Z. H.; Deng, Y. F.; Jiang, Y. Q.; Wan, H. L.; Ng, S. W. *J. Chem. Soc., Dalton Trans.* **2003**, 2636–2638.
- (27) Martell, A. E.; Smith, R. M. *Critical Stability Constants*; Plenum Press: New York, 1974–1977.
- (28) Martell, A. E.; Motekaitis, R. J. *Determination and Use of Stability Constants*; Wiley-VCH: New York, 1992.
- (29) Martell, A. E.; Hancock, R. D. *Metal Complexes in Aqueous Solution*; Plenum Press: New York, 1996.
- (30) Tur'yan, Y. I.; Gnusin, I. N.; Yatsenko, V. I. *Russ. J. Inorg. Chem.* **1978**, *23*, 1145–1147.

In this paper, we address the interaction of Ti(IV) with citrate in aqueous solution. Spectropotentiometric titrations with a range of ligand and metal concentrations afford stability constants and UV/vis spectra for the abundant species formed. From the stability constants, speciation diagrams can be constructed to describe a variety of conditions. Electrospray mass spectrometry provides support for the speciation. Finally, the X-ray crystal structure of the fully deprotonated tris-citrate species $\text{Na}_8[\text{Ti}(\text{cit})_3] \cdot 17\text{H}_2\text{O}$, which crystallizes at pH 7–8, is described.

Experimental Section

Reagents and Chemicals. All aqueous stocks and titration solutions were prepared fresh (for use within one week) with Nanopure-quality water (18.2 M Ω -cm resistivity; Barnstead model D11931). Stock solutions (1.000 M) of KCl and KNO_3 were prepared from ACS-grade crystals (J. T. Baker and Fisher, respectively) by weighing out an appropriate amount of the salt and dissolving it with water in a volumetric flask. Similarly, a 0.1000 M aqueous solution of citric acid was prepared in a volumetric flask from granular citric acid monohydrate (USP-grade, J. T. Baker).

Carbonate-free potassium hydroxide (~0.1 M) was prepared from a 1.0 M stock solution (Dilut-It Analytical Concentrate, J. T. Baker) and standardized by titration against potassium hydrogen phthalate (ACS Primary Standard, Mallinckrodt) using phenolphthalein (1% in 95% alcohol, Mallinckrodt) as an indicator. A Gran's plot analysis^{28,34} was performed to confirm the absence of carbonate (data not shown). Solutions of ~0.1 M hydrochloric acid (1 N Volumetric Solution, J. T. Baker) or nitric acid (15.8 N Certified ACS-grade, Fisher), depending on the supporting electrolyte, were prepared and standardized against KOH, again using phenolphthalein as an indicator. These solutions were used to acidify the titration solutions as necessary.

Preparation of Titration Solutions. Titrations were carried out in either 1.00 or 4.00 mM citrate, and with ligand/metal ratios between 1:1 to 5:1. Titanium(IV) tetrachloride (99.9%, with SureSeal cap, Aldrich) was used as the titanium source for most of the titrations. For a few titrations with a 3:1 ligand/metal ratio, the titanium starting material was a titanium–tris-citrate complex crystallized in our lab from aqueous solution at low pH following the procedure of Zhou et al.²⁶

Titration solutions including supporting electrolyte and citrate ligand (60 mL total volume) were prepared under nitrogen and purged of dissolved gases under vacuum by a freeze–pump–thaw methodology using liquid nitrogen and a Schlenk line. After 3–4 cycles, an appropriate volume of the neat TiCl_4 (2–20 μL) was transferred via a 25- μL gastight glass syringe (Hamilton Co.) to the thawed but cold solution through a rubber septum. Using a volumetric pipet, a 50.0-mL aliquot of the fully prepared titration solution was then transferred to the reaction vessel under argon, and the remaining 10 mL was analyzed for titanium by flame atomic absorption spectroscopy.

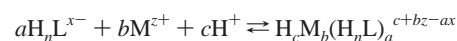
Flame Atomic Absorption Spectrometry. The final titanium concentration was determined by using a Varian SpectrAA-20 flame atomic absorption spectrometer. The standards used to calibrate the

instrument were prepared from a 1000 $\mu\text{g}/\text{mL}$ titanium atomic absorption standard in strong acid (Rikka Chemical Co.). Standards were prepared for each titration to match exactly the citrate (which was found experimentally to suppress the titanium absorption) and the supporting electrolyte concentrations, and to bracket the expected titanium concentration. The instrument was calibrated before and after each sample analysis, and the samples were analyzed in triplicate.

Spectropotentiometric Titrations. All titrations were carried out at 25 °C with stirring and all titration solutions had an initial volume of 50.0 mL. The titration apparatus was constructed according to published methodology²⁸ and consisted of a 100-mL water-jacketed glass vessel (Kontes Co.) attached to a thermostated water bath, and sitting on a magnetic stir-plate. The lid to the titration vessel was machined from $5/8$ -in. plexiglass, with holes drilled for the pH combination electrode, the UV/vis probe, base additions, sampling, and the argon gas (in/out). The holes were fitted with appropriate bushings, connectors, stoppers, and rubber septa, and the lid was sealed to the glass titration vessel by an airtight doughnut-shaped $1/16$ -in. silicon rubber seal (McMaster-Carr Co.).

The pH was monitored as millivoltage readings by using an Orion model 520 pH meter (accurate to 0.1 mV) and an Orion combination pH electrode (model 8102BNU). The electrode was calibrated before and after each titration by measuring voltages when known amounts of KOH were added to a well-characterized 50-mL HCl solution (25 °C in 0.1 M supporting electrolyte) in the pH range 2–11. Resulting pre- and post- calibration Nernst equations were then weighted as a function of time (to account for electrode drift) and used to convert titration voltages to pH.

The equilibrium expressions for all soluble species in a ternary proton-metal ion-ligand equilibrium system can be stated as follows:³⁵



where

$$\beta_{a,b,c}^{\circ} = \frac{\{\text{H}_c\text{M}_b(\text{H}_n\text{L})_a^{c+bz-ax}\}}{\{\text{H}^+\}^c \{\text{M}^{z+}\}^b \{\text{H}_n\text{L}^{x-}\}^a} = \frac{\gamma_{\text{H}_c\text{M}_b(\text{H}_n\text{L})_a^{c+bz-ax}}}{(\gamma_{\text{H}^+})^c (\gamma_{\text{M}^{z+}})^b (\gamma_{(\text{H}_n\text{L})^{x-}})^a} \times \frac{[\text{H}_c\text{M}_b(\text{H}_n\text{L})_a^{c+bz-ax}]}{[\text{H}^+]^c [\text{M}^{z+}]^b [\text{H}_n\text{L}^{x-}]^a}$$

and $\{X\}$ is the activity of X , γ_X is the activity coefficient of X , $[X]$ is the molar concentration of X , and $\beta_{a,b,c}^{\circ}$ is the activity equilibrium constant at zero ionic strength. When the constant ionic strength condition^{28,35,36} is met, whereby a 100-fold excess of noncomplexing supporting electrolyte is added to the titration solution, the activity coefficients of the analytes are essentially held constant and are incorporated into the β -values:

$$\beta_{a,b,c}^{\mu,T}(\text{pH}) = \frac{\beta_{a,b,c}^{\circ}}{\gamma_{\text{H}_c\text{M}_b(\text{H}_n\text{L})_a^{c+bz-ax}}} = \frac{[\text{H}_c\text{M}_b(\text{H}_n\text{L})_a^{c+bz-ax}]}{[\text{H}^+]^c [\text{M}^{z+}]^b [\text{H}_n\text{L}^{x-}]^a} (\gamma_{\text{H}^+})^c (\gamma_{\text{M}^{z+}})^b (\gamma_{(\text{H}_n\text{L})^{x-}})^a$$

where $\beta_{a,b,c}^{\mu,T}$ is the concentration equilibrium constant, μ is the ionic strength, and T is the temperature. These conditional β -values then become functions of concentration, and are customarily

(31) Zolotukhin, V. K.; Gnatyshin, O. M. *Russ. J. Inorg. Chem.* **1973**, *18*, 1467–1470.

(32) Baes, C. F.; Mesmer, R. E. *The Hydrolysis of Cations*; John Wiley & Sons: New York, 1976.

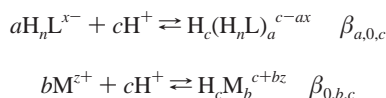
(33) Comba, P.; Merbach, A. E. *Inorg. Chem.* **1987**, *26*, 1315–1323.

(34) Rossotti, F. J.; Rossotti, H. S. *J. Chem. Educ.* **1965**, *42*, 375–378.

(35) Öhman, L. O. *Chem. Geol.* **1998**, *151*, 41–50.

(36) Harris, D. C. *Quantitative Chemical Analysis*; W. H. Freeman: New York, 1999.

reported at a specific ionic strength and temperature, and for a particular supporting electrolyte.^{27,37} The equations can also accommodate binary proton-ligand or proton-metal equilibria



with the understanding that 'c', the coefficient of H⁺ in the above equations, can be a positive or negative number (a negative number implying only that the protons are products of the complexation reaction and not reactants). The potentials then measured are linearly proportional on a logarithmic scale not to the free hydrogen ion activity, A_H, but to the free hydrogen ion concentration, [H⁺]. Since, strictly speaking, pH = -log A_H, it is technically more correct to refer to what is measured with the electrode as p[H⁺], or -log [H⁺]. However, it is accepted practice to refer to this temperature- and ionic strength-dependent quantity as pH.

A positive flow of argon gas was pumped through a wetting solution of supporting electrolyte and then over the experimental solution to preserve the inert atmosphere necessary for these titrations. The concentration of supporting electrolyte (KCl or KNO₃), following tabulated practice,²⁷ was 0.1 M for all titrations. Additions of base were accomplished with a gastight glass syringe (Hamilton Co.), delivered into the titration solution through a rubber septum in volumes ranging from 20 to 500 μL.

Equilibrium was defined to have been reached, following addition of an aliquot of base, when the millivoltage reading remained constant for a minimum of three minutes. This constraint was only a factor in the region near the inflection point (pH ~5–9) where equilibrium took one to several hours to achieve. In this region, the citrate no longer serves as a buffer and the data points are significantly more difficult to record. For a given ligand concentration, this sluggishness was more pronounced as the ligand-to-metal ratio was decreased. Total titration times ranged from several hours for the titration of citric acid alone to several days for ternary proton–titanium–citric acid systems. In addition to potentiometric data, UV/vis spectral data was collected (500–200 nm, 5 nm/sec) on a Cary-50 UV/vis spectrometer (Varian) by using a dip probe (0.2-cm path length) and coupler (Varian parts 79-100326 and 02-101593, respectively). This assembly allowed for the rapid in situ spectroscopic characterization of the titration solution as a function of pH.

Least Squares Fitting. The Fortran program BEST^{28,38} was used to fit experimental potentiometric titration data to calculated curves generated from the optimized group of species proposed in each model. The program uses an algorithm that calculates and refines any number of overlapping log stability constants directly from measured pH values. The function minimized to give a statistical measure of the goodness-of-fit is the sum of the squares of the differences between calculated and observed pH values. By working iteratively between cycles of refinement and optimization, numerous models can be compared, and the stability constants that most accurately describe the system can be estimated. An accompanying Fortran program, SPE,²⁸ that extracts information directly from the fitting program BEST, was used to display pH-dependent species distributions from given log stability constants.

Although *d*–*d* transitions are precluded in the case of the *d*⁰ metal Ti(IV), on complexation with citrate some fairly strong putative ligand-to-metal charge-transfer absorptions (ε ~6000

M⁻¹cm⁻¹) can be seen in the region between 250 and 310 nm. On the basis of this observation, pH-dependent UV/vis spectroscopic scans were collected for the titrations, as described above, and the program Specfit/32^{39–43} was used to model the experimental data. An algorithm designated model-free evolving factor analysis (EFA) was used to estimate, independent of any model, the number of significant eigenvectors or factors (corresponding to different colored species) in each multivariate 3D data set, and their relative contributions as a function of pH. The putative species corresponding to the significant factors were then fitted to the ternary metal–ligand–proton speciation models that were proposed and refined for the potentiometric data. For the purposes of this investigation, the spectral fits were used to confirm the potentiometric speciation described above.

Synthesis of Na₈[Ti(C₆H₄O₇)₃]·17H₂O (1). A purple Ti(III) citrate solution was prepared by the addition of 13 mL of 0.5 M sodium citrate (Na₃C₆H₅O₇·2H₂O, ACS-grade, Alfa-Aesar) solution (6.48 mmol) to TiCl₃ (0.5 g, 3.24 mmol, Aldrich) under N₂. The solution was then air-oxidized to generate Ti(IV) citrate in situ. The pH was increased to 7 using NaOH. Crystals were grown from diffusion of methanol into the aqueous Ti(IV) citrate solution at 4 °C. Yield: 0.536 g (22.5%). CH elemental analysis for C₁₈H₄₆O₃₈·Na₈Ti. Found (calcd): C 19.59% (19.6%), H 4.17% (4.05%). IR (KBr disk) (cm⁻¹): ν_{as}(CO₂) 1653, 1576; ν_s(CO₂) 1440, 1361; ν(Ti–O) 692, 654. ¹H NMR δ_H(D₂O): 2.438 (d, J = 17.2 Hz, CH₂), 2.575 (d, J = 17.2 Hz, CH₂) ppm.

Physical Measurements. Infrared spectra were recorded in the form of a KBr disk by using a Midac FT-IR spectrometer. ¹H NMR spectra were recorded on a Bruker Avance 400 MHz spectrometer in D₂O using sodium 2,2-dimethyl-2-silapentane-5-sulfonate as an internal reference. The electrospray mass spectrum of the aqueous solution of complex **1** was collected on a Waters/Micromass ZQ spectrometer at a capillary voltage of 3 kV, cone voltage of ~45 V, and extractor voltage of 3 V. Elemental analysis was performed by Atlantic Microlabs (Norcross, Georgia).

X-ray Structure Determination. A colorless plate crystal of **1**, having approximate dimensions of 0.25 × 0.25 × 0.10 mm³, was mounted with epoxy cement onto the tip of a fine glass fiber. All measurements were made on a Nonius Kappa CCD diffractometer with graphite monochromated Mo Kα radiation. The data were collected at a temperature of 173(2) K to a maximum 2θ value of 57.32°. The data frames were scaled and processed using the DENZO software package.⁴⁴ The data were corrected for Lorentz and polarization effects and no absorption correction was applied. A total of 16679 reflections were collected, of which 9836 were unique and observed (R_{int} = 0.0249). The structure was solved by direct methods and expanded using Fourier techniques.⁴⁵ The non-hydrogen atoms were refined anisotropically, and hydrogen atoms, with the exception of hydrogens associated with disordered Na(7) and Na(8), were located from electron difference map and refined with isotropic displacement parameters. Relevant crystallographic data appear in Table 1.

(37) Hogfeldt, E. *Stability Constants of Metal-Ion Complexes. Part A: Inorganic Ligands*; Pergamon Press: Oxford, 1982; Vol. 21.

(38) Motekaitis, R. J.; Martell, A. E. *Can. J. Chem.* **1982**, *60*, 2403–2409.

(39) Binstead, R. A.; Jung, B.; Zuberbühler, A. D. *Specfit/32*; Software Associates: Marlborough, MA, 2001.

(40) Gampp, H.; Maeder, M.; Meyer, C. J.; Zuberbühler, A. D. *Talanta* **1985**, *32*, 95–101.

(41) Gampp, H.; Maeder, M.; Meyer, C. J.; Zuberbühler, A. D. *Talanta* **1985**, *32*, 257–264.

(42) Gampp, H.; Maeder, M.; Meyer, C. J.; Zuberbühler, A. D. *Talanta* **1985**, *32*, 1133–1139.

(43) Gampp, H.; Maeder, M.; Meyer, C. J.; Zuberbühler, A. D. *Talanta* **1986**, *33*, 943–951.

(44) Otwinowski, Z.; Minor, W. *Methods Enzymol.* **1997**, *276*, 307–326.

(45) Sheldrick, G. M. *Acta Crystallogr.* **1990**, *A46*, 467–473.

Table 1. Crystallographic Data for $\text{Na}_8[\text{Ti}(\text{C}_6\text{H}_4\text{O}_7)_3] \cdot 17\text{H}_2\text{O}$ (1)

chemical formula	$\text{C}_{18}\text{H}_{46}\text{Na}_8\text{O}_{38}\text{Ti}$
formula weight	1102.37
a (Å)	11.634(2)
b (Å)	13.223(3)
c (Å)	13.291(3)
α (deg)	99.27(3)
β (deg)	92.21(3)
γ (deg)	99.95(3)
V (Å ³)	1982.9(7)
Z	2
space group	$P\bar{1}$
T (K)	173(2)
λ	Mo K α , 0.71073 Å
D_{calcd} (g cm ⁻³)	1.846
μ (cm ⁻¹)	4.30
R^a	0.0575 ^b
R_w^a	0.1748 ^b

^a R values are based on F ; R_w values are based on F^2 . $R = \sum ||F_o| - |F_c|| / \sum |F_o|$, $R_w = \{ \sum [w(F_o^2 - F_c^2)^2] / \sum [w(F_o^2)^2] \}^{1/2}$. ^b For 9836 reflections with $I > 2\sigma(I)$.

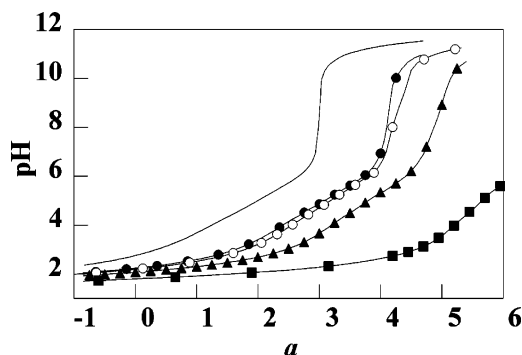


Figure 1. Potentiometric titration curves for 4.00 mM citric acid in the presence of various concentrations of titanium(IV) at 25 °C and 0.1 M KCl. The value on the x-axis, a , represents the net moles of base added (KOH) per mole of ligand.²⁸ Data are as follows: no symbol, citrate alone with no titanium; closed circles (●), [Ti] = 0.98 mM (ligand-to-metal ratio of 4.1:1); open circles (○), [Ti] = 1.33 mM (L:M ratio 3.0:1); triangles (▲), [Ti] = 1.56 mM (L:M ratio 2.6:1); squares (■), [Ti] = 3.30 mM (L:M ratio 1.2:1). For clarity, in each case, only every fifth collected data point is shown.

Results

Spectropotentiometric Titrations. In the absence of a Lewis acid such as Ti(IV), the titration of citric acid with strong base (KOH) in 0.1 M KCl and at 25 °C followed a course characteristic of a triprotic acid, with three equiv of base necessary to reach the inflection point (Figure 1). The fitting program BEST was used to determine the experimental pK_a s for the three carboxyl protons from the potentiometric data, and the results were in agreement with tabulated values.²⁷ When the same titration was done in the presence of various concentrations of Ti(IV) in an argon environment, the resulting curves were shifted to lower pH for a given amount of added base, indicating the displacement of protons from the ligand by the metal.

It can be seen in Figure 1 that, at ligand/metal ratios near 3:1, four equiv of base are necessary to fully deprotonate the citric acid in aqueous solution. This result is an indication that, in addition to the three carboxyl protons, the α -hydroxyl proton on the citrate ligand is ionized in the presence of Ti(IV). In the absence of Ti(IV), the pK_a for this proton is > 14 , and is not amenable to aqueous electrode potentiometry.

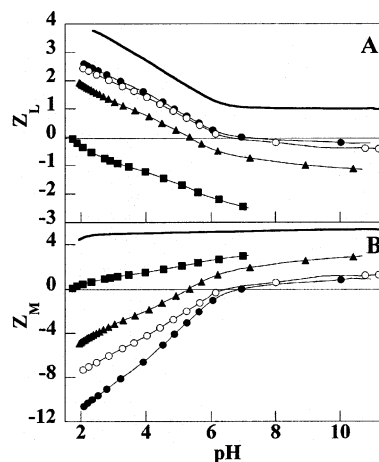


Figure 2. Experimental deprotonation curves for 4.00 mM citric acid in the presence of various concentrations of Ti(IV) at 25 °C and 0.1 M KCl. (A) Z_L represents the number of protons bound per ligand as a function of pH (assumes H_4L -type ligand). Data are as follows: no symbol, citrate alone with no titanium; closed circles (●), [Ti] = 0.98 mM (ligand-to-metal ratio of 4.1:1); open circles (○), [Ti] = 1.33 mM (L:M ratio 3.0:1); triangles (▲), [Ti] = 1.56 mM (L:M ratio 2.6:1); squares (■), [Ti] = 3.30 mM (L:M ratio 1.2:1). For clarity, in each case, only every fifth collected data point is shown. (B) Z_M represents the number of hydroxides bound per metal atom. Data are as follows: no symbol, 1.84 mM Ti with no citrate; other symbols as in Figure 2A.

It can also be inferred from Figure 1 that at ligand/metal ratios below 3:1, more than four equiv of base are needed to reach the inflection point. Because there are only four ionizable protons per citrate molecule, the additional free protons can only be generated hydrolytically by the binding of hydroxide ion(s) to Ti(IV), with the concomitant liberation of proton(s). Significantly, it was found that during the course of the titrations (pH range 2–11), even at ligand/metal ratios below 3:1, no precipitate was observed. In the absence of a stabilizing complexation ligand like citrate, the potent Lewis acid Ti(IV) forms a hydrolytic precipitate in aqueous solution at acidities below pH 3 (data not shown), putatively $\text{TiO}(\text{OH})_2^{46}$ or $\text{Ti}(\text{OH})_4$.³²

The Z_L and Z_M curves (Figure 2) are functions of pH and were used to visualize the number of protons bound per ligand or the number of hydroxides bound per metal, respectively. The following were adapted from Öhman:^{35,47}

$$Z_L(\text{pH}) = \frac{[\text{H}_{\text{bound}}]}{[\text{cit}_{\text{total}}]}$$

$$Z_M(\text{pH}) = \frac{-[\text{H}_{\text{bound}}]}{[\text{Ti(IV)}_{\text{total}}]}$$

where

$$[\text{H}_{\text{bound}}] = [\text{H}_{\text{total}}] - [\text{H}_{\text{free}}]$$

and

$$[\text{H}_{\text{total}}] = [x\text{sH}] + 4[\text{cit}_{\text{total}}] - [\text{OH}_{\text{added}}]$$

The quantities $[\text{cit}_{\text{total}}]$, $[\text{Ti(IV)}_{\text{total}}]$, $[x\text{sH}]$, and $[\text{OH}_{\text{added}}]$ are

(46) Einaga, H.; Komatsu, Y. *J. Inorg. Nucl. Chem.* **1981**, *43*, 2443–2448.

(47) Öhman, L. O.; Sjöberg, S. *Coord. Chem. Rev.* **1996**, *149*, 33–57.

known (x_sH being the excess concentration of strong acid added, if any), and $[H_{\text{free}}]$ is measured as pH. In both panels a “zero-line” was inserted to make the interpretation more straightforward. In Figure 2A, the zero-line represents the limit of titratable protons for a tetraprotic acid, and when the function becomes negative, mixed hydroxo–Ti(IV)–citrate complexes are indicated. In a similar fashion, when the function becomes positive in Figure 2B, hydrolytic binding of hydroxide ion is indicated.

The Z_L curve (Figure 2A) for the titration of citric acid alone reinforces the experimental observation that, in the absence of Ti(IV), the α -hydroxyl proton is not ionized, and the acid is essentially triprotic in the pH range 2–11. The Z_L curves for citric acid in the presence of Ti(IV), however, particularly those for which the ligand/metal ratio is 3:1 or greater, are shifted almost uniformly to lower pH, with deprotonation of the carboxylic acid moieties following a nearly identical course. This result is further evidence that the α -hydroxyl proton is indeed ionized in the presence of Ti(IV), since these curves are shifted by approximately one proton throughout the course of the titration.

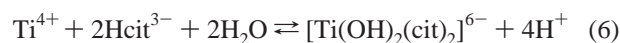
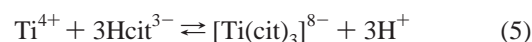
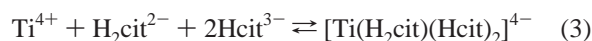
The Z_M curves (Figure 2B) reveal the extent of hydroxide binding to the metal, because they are referenced to the metal concentration. Thus, at ligand/metal ratios of 3:1 or greater, no net hydroxide binding occurs until pH \sim 7, and an average of approximately one hydroxide is bound per metal ion at the limit of the titration (pH \sim 11). At a ligand/metal ratio of 2.6:1, no net hydrolysis is observed until pH \sim 5, and an average of three hydroxides are bound to the metal by pH \sim 10, while at a ligand/metal ratio of 1.2:1, an average of three hydroxides are bound at pH \sim 7, and hydrolysis begins at a pH below 2. Finally, in the titration of Ti(IV) with no citrate, the metal immediately hydrolyzes more than four water molecules, on average, and precipitation begins below pH 3.

Focusing on titrations with at least a 3-fold excess of citrate, UV/vis scans and pH readings were collected point-for-point in a titration of 3.8 equiv of citric acid with 1 equiv of Ti(IV). The spectral data are presented in Figure 3 as difference spectra. Each scan was corrected for dilution, and the $\nu = 0$ mL titration point (pH 2.314) scan was subtracted from each. In the region between pH 2.3 and 3.4, an absorption band grows in with a $\lambda_{\text{max}} \sim 272$ nm (Figure 3A). This band subsides and shifts to slightly lower energy ($\lambda_{\text{max}} \sim 278$ nm at pH 5.5) in Figure 3B and C (pH 3.4–5.5), then increases sharply in two phases between pH 5.5 and 7.0 and pH 7.0 and 9.1 (Figure 3D and E), with a $\lambda_{\text{max}} \sim 266$ nm at pH 9.1. Finally, the absorption decreases with a further shift to higher energy in the pH range 9.1–10.9 (Figure 3F). Spectral data collected for the identical titrations of ligand alone and metal alone do not show these absorptions (data not shown). Model-free EFA, performed on the raw spectral data using the Specfit/32 software, identified six significant eigenvectors corresponding to abundant colored species, with concentration maxima at approximately pH 2.0, 3.0, 4.5, 5.5, 6.5, and 9.5.

Several conclusions were then drawn concerning titrations with at least a 3-fold excess of ligand, namely: (1) citric

acid behaves like a tetraprotic acid in the presence of Ti(IV), where (2) one citrate proton is ionized at low pH (\sim 2) and three others before pH 7 ($H_3\text{cit}$ $pK_{\text{a}s}$ at 0.1 M ionic strength: 2.90, 4.35, 5.67);²⁷ (3) above pH \sim 7 some hydrolytically driven binding of Ti(IV) by hydroxide ion occurs; and (4) there are at least six abundant Ti(IV)–citrate species involved in the experimental pH range 2–11. These observations were then used, in conjunction with the potentiometric fitting program BEST, to refine and test potential speciation models.

Various models describing equilibrium systems with 1:1 complexes only, with 2:1 complexes only, and with 3:1 complexes only were tested, as well as systems with varying number of total species and mixed ratios (some 1:1, some 2:1 etc.). Models invoking only hydrolytic titanium hydroxide species were also tested, as were models involving dimers and models involving ternary Ti(IV)–citrate–hydroxide species. Two species consistently improved their respective fits when proposed in a model, and did not violate the guiding considerations mentioned above: a 1:1 complex occurring at low pH, and a mixed 2:1 complex occurring at high pH. In the region between the two, models that best fit the data consistently rejected all but four species, and models proposing dimer formation, titanium hydroxide species, or mixed ratios did not improve fits in any combination. Furthermore, models proposing a series of 3:1 complexes fit the data better than models proposing only 2:1 or 1:1 complexes (see Supporting Information for a comparison of representative least-squares fits of the data). Ultimately, the model that most closely fit the potentiometric data comprised the following equilibrium system:

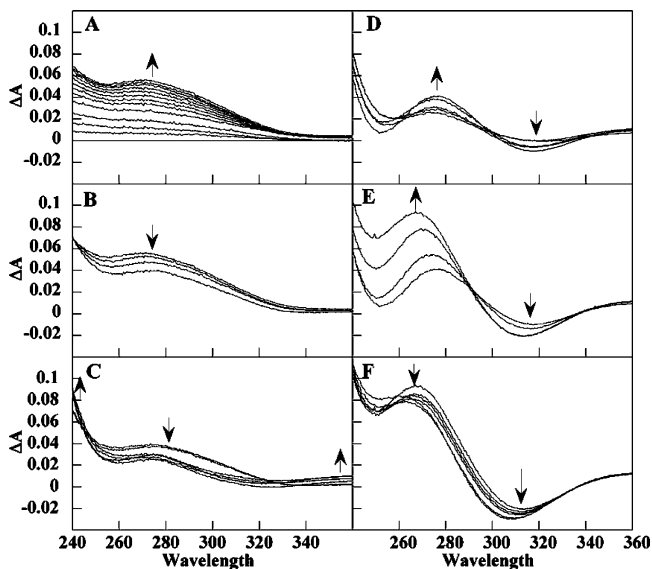


The optimized least-squares fit of the data based on these equilibria, which necessarily included the three measurable protonation constants of citric acid and the pK_w (13.79 at 0.1 M ionic strength), generated $\log \beta$ values that are reported in Table 2, along with expressions describing the equilibria presented in the format recommended by Martell and Smith.²⁷

When the stability constants determined for the above model were used to fit other potentiometric titration data for systems with a ligand/metal ratio greater than three, similar optimal fits were obtained, whether the starting ligand concentration was 1.00 mM or 4.00 mM, and whether the supporting electrolyte was KCl or KNO_3 (data not shown). Conversely, for those titrations where the ratio was less than three, the fits of the same model were not robust or

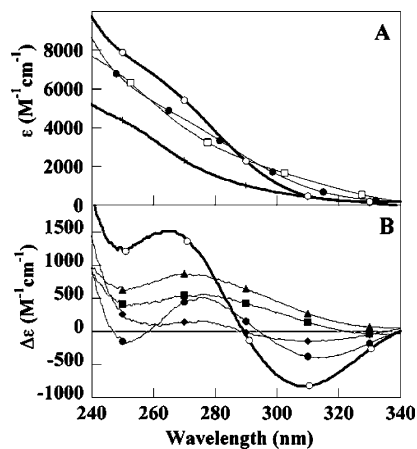
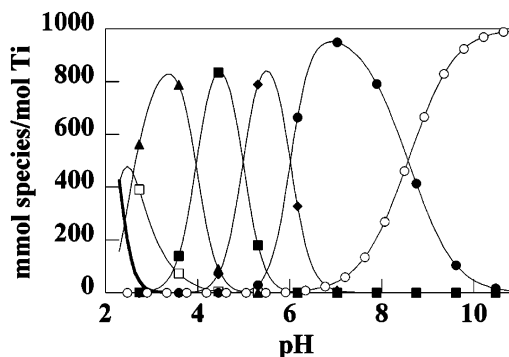
Table 2. Stability Constants (β -Values) for Aqueous Ti(IV)–Citrate Species (0.1 M KCl, 25 °C, Argon Atmosphere)^a

eq	equilibrium expression	log β
1	$[M(HL)]/[M][HL]$	9.18
2	$[M(H_2L)_3]/[M][H_2L]^3$	16.99
3	$[M(H_2L)(HL)_2]/[M][H_2L][HL]^2$	20.41
4	$[M(HL)_2L]/[H]/[M][HL]^3$	16.11
5	$[ML_3][H]^3/[M][HL]^3$	4.07
6	$[M(OH)_2L_2][H]^4/[M][HL]^2$	-7.94

^a Charges are omitted for clarity.**Figure 3.** Selected UV/vis difference spectra for a spectropotentiometric titration of 1.00 mM citrate and 0.26 mM Ti(IV) (3.8:1 ligand/metal ratio) at 25.0 °C and 0.1 M KCl. The spectra were corrected for dilution, and the spectrum at pH 2.3 was subtracted from each to emphasize optical changes. Ranges were (A) pH 2.3–3.4, (B) pH 3.4–4.5, (C) pH 4.5–5.5, (D) pH 5.5–7.0, (E) pH 7.0–9.1, and (F) pH 9.1–10.9.

reproducible, and could not be improved without severe alteration of the model (data not shown), either by eliminating all 3:1 species or by invoking many extra mixed-hydroxo species.

The speciation model (species and β -values) was then applied to the complementary spectroscopic data, and the absorbance spectra for the species in the model are presented in Figure 4. Figure 4A reveals the range of extinction coefficients ($\epsilon \sim 4000\text{--}6000 \text{ M}^{-1}\text{cm}^{-1}$) at the wavelengths of interest (260–280 nm), and their magnitude, although part of a shoulder in the spectrum and therefore difficult to quantify, is indicative of a charge transfer, presumably a ligand-to-metal charge transfer (LMCT). In Figure 4B, presented as difference spectra, each trace has had the trace of the 1:1 complex subtracted from it, since, according to the species distribution, this species dominates at the beginning of the titration (see below). The absorptions of the titanium–tris-citrate species in the region between 260 and 280 nm decrease as protons are removed, until the absorption sharply increases when the fully deprotonated species begins to grow in at pH ~ 6 . There is also a steady decline in absorption at lower energy (300–320 nm) as protons are removed from the ligands. As the titration solution becomes more basic (pH > 8), the mixed hydroxo-species begins to dominate the absorption spectrum.

**Figure 4.** UV/vis spectra generated from spectropotentiometric titration of 3.8:1 citrate/Ti(IV) by using Specfit.³⁹ (A) UV/vis spectra for each species: crosses (+), $\text{Ti}^{4+}(\text{aq})$; open squares (\square), $[\text{Ti}(\text{Hcit})]^+$; closed circles (\bullet), $[\text{Ti}(\text{cit})_3]^{8-}$; open circles (\circ), $[\text{Ti}(\text{OH})_2(\text{cit})_2]^{6-}$. (B) Difference spectra with $[\text{Ti}(\text{Hcit})]^+$ spectrum subtracted from each: triangles (\blacktriangle), $[\text{Ti}(\text{H}_2\text{cit})_3]^{2-}$; squares (\blacksquare), $[\text{Ti}(\text{H}_2\text{cit})(\text{Hcit})_2]^{4-}$; diamonds (\blacklozenge), $[\text{Ti}(\text{Hcit})_2(\text{cit})]^{6-}$; closed circles (\bullet), $[\text{Ti}(\text{cit})_3]^{8-}$; open circles (\circ), $[\text{Ti}(\text{OH})_2(\text{cit})_2]^{6-}$.**Figure 5.** Speciation diagram for Ti(IV)-containing species generated by program SPE²⁸ from best fit β values for 3.8:1 citrate/Ti(IV). Species are: no symbol with bold line, $\text{Ti}^{4+}(\text{aq})$; open squares (\square), $[\text{Ti}(\text{Hcit})]^+$; triangles (\blacktriangle), $[\text{Ti}(\text{H}_2\text{cit})_3]^{2-}$; squares (\blacksquare), $[\text{Ti}(\text{H}_2\text{cit})(\text{Hcit})_2]^{4-}$; diamonds (\blacklozenge), $[\text{Ti}(\text{Hcit})_2(\text{cit})]^{6-}$; closed circles (\bullet), $[\text{Ti}(\text{cit})_3]^{8-}$; open circles (\circ), $[\text{Ti}(\text{OH})_2(\text{cit})_2]^{6-}$. Free ligand species are omitted for clarity.

A species distribution diagram was generated from the speciation model (Figure 5), and when compared to the spectroscopic data presented in Figure 3, several observations can be made. The region described in Figure 3A (pH 2.3–3.4) coincides with the increasing concentration of the first titanium–tris-citrate species, $[\text{Ti}(\text{H}_2\text{cit})_3]^{2-}$ in the same region as in Figure 5. The two intermediate species, $[\text{Ti}(\text{H}_2\text{cit})(\text{Hcit})_2]^{4-}$ and $[\text{Ti}(\text{Hcit})_2(\text{cit})]^{6-}$, have concentration maxima at approximately pH 4.5 and 5.5, respectively, and are represented optically in the decreasing absorption band at $\sim 275 \text{ nm}$ (Figure 3B and C). The fully deprotonated species, $[\text{Ti}(\text{cit})_3]^{8-}$, grows in sharply in the pH range 5.5–7.0, at approximately the same energy (Figure 3D) as the other titanium–tris-citrate complexes. This result is consistent with the concentration profile of this species in Figure 5. The mixed species, $[\text{Ti}(\text{OH})_2(\text{cit})_2]^{6-}$, which according to Figure 5 begins to form in significant amount in solution above pH ~ 7 , becomes the dominant species in solution at pH ~ 9 . The absorbance of this species is reflected in the difference spectra shown in Figure 3E and F, in which there is a shift

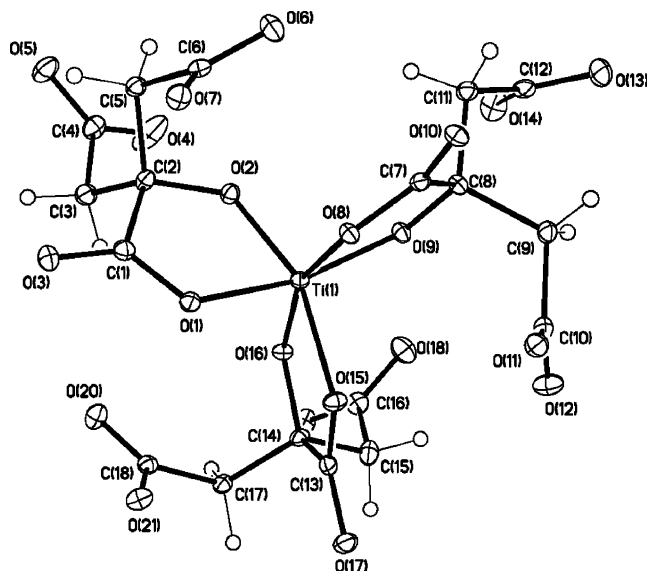


Figure 6. ORTEP plot, with atom-labeling scheme, of the complex anion $[\text{Ti}(\text{C}_6\text{H}_4\text{O}_7)_3]^{8-}$ in **1** at the 30% probability level.

Table 3. Selected Bond Lengths (Å) and Angles (deg) for the Complex Anion $[\text{Ti}(\text{C}_6\text{H}_4\text{O}_7)_3]^{8-}$ from **1**

Ti—O(9)	1.8330(18)	O(2)—Ti—O(1)	79.49(8)
Ti—O(2)	1.8542(18)	O(16)—Ti—O(1)	101.77(8)
Ti—O(16)	1.8613(18)	O(9)—Ti—O(8)	78.43(8)
Ti—O(1)	2.0058(18)	O(2)—Ti—O(8)	104.89(8)
Ti—O(8)	2.0730(18)	O(16)—Ti—O(8)	158.28(8)
Ti—O(15)	2.0762(18)	O(1)—Ti—O(8)	81.11(8)
O(9)—Ti—O(2)	97.71(9)	O(9)—Ti—O(15)	103.96(8)
O(9)—Ti—O(16)	100.35(8)	O(2)—Ti—O(15)	158.29(8)
O(2)—Ti—O(16)	96.78(8)	O(16)—Ti—O(15)	78.20(8)
O(9)—Ti—O(1)	157.88(8)	O(1)—Ti—O(15)	80.90(8)
		O(8)—Ti—O(15)	81.06(8)

to higher energy and stronger absorption in the pH range 7.0–10.9.

Description of the Crystal Structure of $\text{Na}_8[\text{Ti}(\text{C}_6\text{H}_4\text{O}_7)_3] \cdot 17\text{H}_2\text{O}$ (1**).** Complex **1** crystallizes in a triclinic $P\bar{1}$ space group with two molecules in the unit cell. The ORTEP diagram for the complex anion of **1** is shown in Figure 6, and selected bond distances and angles are shown in Table 3. The complex has a distorted octahedral geometry and is solvated by 17 waters of crystallization. The majority of the complex is fully resolved with the exception of two sodium atoms, Na(7) and Na(8), and the carboxylate arm of one of the citrates. The sodium atoms were modeled in two possible locations with occupancy factor ratios of 65:35 and 50:50 for Na(7/7') and Na(8/8'), respectively. The C(16) and O(18) of the carboxylate arm were modeled with an occupancy factor ratio of 80:20 and refined with anisotropic displacement parameters.

The X-ray crystal structure of **1** shows titanium bound to three citrates where each of the citrates is acting as a bidentate ligand, chelating through the α -hydroxyl and α -carboxyl oxygens. A similar α -hydroxy acid chelation mode is observed in complexes of other metals such as Al(III)⁴⁸ and Fe(III),¹⁶ although in these cases the additional binding of a dangling carboxylate is also observed. At pH 7, the three

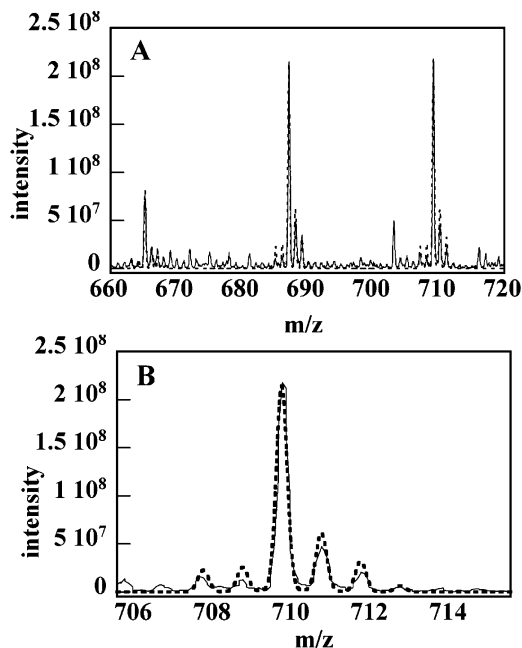


Figure 7. Electrospray mass spectrum (positive ion mode). (A) Mass range showing peaks consistent with titanium isotope distributions for $\text{Na}_3[\text{Ti}(\text{H}_2\text{-cit})_3]^+$ (peaks $\sim m/z = 690$), $\text{Na}_2\text{H}[\text{Ti}(\text{H}_2\text{cit})_3]^+$ (peaks $\sim m/z = 665$) and $\text{Na}_4[\text{Ti}(\text{H}_2\text{cit})_2(\text{Hcit})]^+$ (peaks $\sim m/z = 710$). (B) Expansion of the latter region, showing the data and model (dashed line).

citrate are completely deprotonated, giving the overall complex a high anionic charge which is balanced by eight sodium ions. With this type of coordination several isomers are possible. The hydroxyl oxygens of the three citrates lie on the same face of the octahedron giving the facial isomer. Also, there is an opportunity to exhibit optical isomerism and Figure 6 depicts the Δ isomer.

FT-IR Spectroscopy. The FT-infrared spectrum shows well-resolved sharp carbonyl asymmetric and symmetric stretches. The asymmetric stretches appear between 1653 and 1576 cm^{-1} and the corresponding symmetric stretches appear between 1440 and 1361 cm^{-1} , similar to where they appear in the related complexes at lower pH.²⁶ The difference between the asymmetric and symmetric stretches is $\sim 200 \text{ cm}^{-1}$ suggesting free carboxylates or those that are bound in a monodentate fashion.⁴⁹ This finding is in agreement with the X-ray crystal structure of **1**.

^1H NMR Spectroscopy. ^1H NMR of **1** in D_2O shows four sets of doublets that are coupled to each other such that only 7 peaks are observed, which suggests that in solution some of the Ti(IV) citrate dissociates to give free citrate. This result is in agreement with an earlier report in which solution NMR for $(\text{NH}_4)_2[\text{Ti}(\text{H}_2\text{cit})_3]$ also showed peaks associated with free citrate.²⁵

Electrospray Mass Spectrometry. The electrospray mass spectrum of crystals of **1** dissolved in water confirms the existence of several 3:1 species in solution. Some of the dangling carboxylates are protonated in the instrument. This result is consistent with the speciation data. Figure 7 shows a species isotope model overlaid on the experimental spectrum.

(48) Matzapetakis, M.; Raptopoulou, C. P.; Terzis, A.; Lakatos, A.; Kiss, T.; Salifoglou, A. *Inorg. Chem.* **1999**, *38*, 618–619.

(49) Deacon, G. B.; Phillips, R. J. *Coord. Chem. Rev.* **1980**, *33*, 227–250.

Discussion

The tabulated log stability constants for the 1:1 complexes formed by the hard ligand citrate (HL^{3-}) with several groups of metal ions can be compared directly to the value reported above for the complex $[\text{Ti}(\text{Hcit})]^+$. The borderline hard–soft divalent first-row transition metal ions from manganese to zinc form 1:1 citrate complexes whose log β values follow the trend postulated in the Irving–Williams series,⁵⁰ with average reported values (0.1 M ionic strength, 25 °C) ranging from 3.8 for Mn(II) to a high of 5.9 for Cu(II) and 4.8 for Zn(II).²⁷ The hard trivalent lanthanide metal ions form 1:1 complexes with citrate with log stability constants ranging from 7.1 for La(III) to 8.1 for Lu(III) under the same conditions.²⁷ The value reported here (log $\beta = 9.18$) for the 1:1 complex of citrate with the tetravalent Ti(IV) ion can then be rationalized with reference to hard–soft theory, according to which the hard metal ion Ti(IV) should form a 1:1 citrate complex whose stability is more similar in magnitude to the hard trivalent lanthanides than to the borderline divalent first-row transition metals. It can be further reasoned that Ti(IV), with a charge-to-size ratio considerably higher than that of the trivalent lanthanides, should form a 1:1 complex with citrate, bearing as it does only hard carboxylato- or alkoxo- functionalities, that is even more stable (more positive log β value) than the corresponding values for the lanthanides. In accord with this reasoning, the current stability value agrees closely with values for the very similar ions Al(III) (log $\beta = 7.98$) and Fe(III) (log $\beta = 11.2$).²⁷

A similar line of reasoning could not be applied to the titanium(IV)–tris-citrate species that are reported here because there are no published metal ion–tris-citrate benchmarks. However, it is important to note that, for a given speciation model, the magnitude of the stability constants dictates the pH range at which species will appear, with those having significantly higher log β values appearing at low pH and those having significantly lower log β values appearing only at high pH. This statement reflects the competition of Ti(IV) with protons for ligand binding sites. The current speciation model, independently derived, suggests that the crystallized tris-citrate complexes do reflect the dominant species in solution at each pH of crystallization. In particular, $[\text{Ti}(\text{H}_2\text{cit})_3]^{2-}$ was crystallized between pH 1 and 2.8,^{25,26} $[\text{Ti}(\text{H}_2\text{cit})(\text{Hcit})_2]^{4-}$ crystallized between pH 2.8 and 4,²⁵ and $[\text{Ti}(\text{cit})_3]^{8-}$ crystallized at pH 7–8 in the current work. The stability of these Ti(IV)–tris-citrate complexes as reflected in the log stability constants is consistent with the possibility that citrate may accelerate the dissolution of environmental titanium-containing materials. Citrate may also scavenge aqueous Ti(IV) in biological systems such as in human plasma, where citrate reaches concentrations of ~ 0.1 mM.⁶

Several well-characterized transition metal citrate complexes of di- or higher nuclearity are known, such as the one with Fe(III).⁵¹ From aqueous solution, typically at neutral pH values of 7–8, mononuclear citrate complexes of Mn-

(II),¹⁵ Co(II),¹⁷ Ni(II),¹⁸ Cu(II),¹⁹ and Zn(II)²⁰ crystallize in the form $[\text{M}(\text{Hcit})_2]^{4-}$. These complexes feature two tridentate coordinating citrates, each binding with one bidentate α -hydroxy acid and one β -carboxylate, leaving two dangling β -carboxylates, one from each citrate. In some complexes, a proton was assigned to the hydroxy oxygen on each coordinating citrate, so that the dangling citrates were each deprotonated. Fully deprotonated citrate complexes with the harder metals Al(III) and Ga(III),²¹ Fe(III)¹⁶ and Mn(III)¹⁵ ($[\text{M}(\text{cit})_2]^{5-}$) crystallized from aqueous solution around the same pH. A similar bis-citrate complex with Cr(III) was crystallized as a 2- species from an aqueous solution of indeterminate pH.⁵² Mononuclear Al(III) or Ga(III) bis-citrate compounds crystallized from aqueous solution at pH 4.5 reflected a proton on just one of the two citrates, giving a complex of the form $[\text{M}(\text{cit})(\text{Hcit})]^{4-}$.²¹ Coordination of three citrates to one metal, as noted above, or dangling of both β -carboxylates, is not observed in any of these complexes.

Of the compounds crystallographically characterized thus far, only Ti(IV) gives mononuclear tris-citrate species that do not coordinate through the β -carboxylates, although these carboxylates do coordinate in the Ti(IV) species of higher nuclearity.^{23,24} This observation cannot be attributed to the size of the metal, a point which can be illustrated by comparing Ti(IV) to similarly hard Lewis acidic metals for which 2:1 citrate/metal complexes are observed. Al(III) has an effective ionic radius of 0.535 Å, while high spin Fe(III) has an ionic radius of 0.645 Å. Ti(IV) falls in the middle, with an ionic radius of 0.605 Å.⁵³ The metal to hydroxyl oxygen bond distances for the mononuclear citrate complexes of these three metals follow the same trend, with 1.844 Å for Al(III),⁴⁸ averaging 1.850 Å for $[\text{Ti}(\text{IV})(\text{cit})_3]^{8-}$, and 1.953 Å for Fe(III).¹⁶ This bond distance for the lower pH, more highly protonated forms of Ti(IV) tris-citrate exhibit bond distances ranging from 1.848 to 1.874 Å, also within this range.^{25,26}

The trends in bond distance to the α -carboxylate oxygens are more complicated. In addition, it is important to note that some of these complexes have different counterions, which may influence the observed bond distances somewhat. Of the citrate complexes crystallized at pH 7–8, the bond distances to the α -carboxylate oxygens are longest for the Ti(IV) complex, perhaps because three citrate ligands are crowded around the metal. The distances are 1.884 Å for Al(III),⁴⁸ averaging 2.052 Å for Ti(IV), and 2.008 Å for Fe(III).¹⁶ For the lower pH forms of Ti(IV) tris-citrate, the distances are somewhat shorter (averaging 2.007 Å) for the $[\text{Ti}(\text{H}_2\text{cit})(\text{Hcit})_2]^{4-}$ species, which exhibits strong hydrogen bonding among the protonated and deprotonated dangling carboxylates.²⁵ The $[\text{Ti}(\text{H}_2\text{cit})_3]^{2-}$ complexes show average bond distances of 2.047 Å,²⁶ more similar to that seen in $[\text{Ti}(\text{cit})_3]^{8-}$. Distances to the β -carboxylate oxygens, which coordinate only for the Al(III) and Fe(III) species, are longer

(50) Irving, H.; Williams, R. J. *Chem. Soc.* **1953**, 3192–3210.

(51) Shweky, I.; Bino, A.; Goldberg, D. P.; Lippard, S. J. *Inorg. Chem.* **1994**, *33*, 5161–5162.

(52) Quiros, M.; Goodgame, D. M. L.; Williams, D. J. *Polyhedron* **1992**, *11*, 1343–1348.

(53) Shannon, R. D. *Acta Crystallogr.* **1976**, *A32*, 751–767.

than those to the α -carboxylates: 1.961 and 2.068 Å, respectively.^{16,48}

Each of the nearly octahedral tris-citrate complexes crystallographically characterized thus far occurs with three hydroxyl oxygen atoms on the same face of the octahedron.^{25,26} With three bidentate ligands, the complexes can exhibit either Λ or Δ isomerism at the metal center.⁵⁴ Figure 6 depicts the Δ isomer, but the $P\bar{1}$ space group, with its center of inversion, contains two molecules in the unit cell, one of each configuration.

It is important to note that titanium compounds are quite labile. Using water exchange as a standard benchmark, the rate constant for exchange in the Ti(III) species $[\text{Ti}(\text{H}_2\text{O})_6]^{3+}$ is $1.8 \times 10^5 \text{ s}^{-1}$ at room temperature,⁵⁵ and a lower limit of $3.4 \times 10^3 \text{ s}^{-1}$ has been placed on the exchange of terminal water ligands in oligomeric hydrolyzed Ti(IV) solutions.³³ These values can be compared to rate constants for exchange of $1.6 \times 10^2 \text{ s}^{-1}$ for $[\text{Fe}(\text{H}_2\text{O})_6]^{3+}$ and 2.4×10^{-6} for the famously inert $[\text{Cr}(\text{H}_2\text{O})_6]^{3+}$.⁵⁶

The electrospray mass spectrometry data as shown in Figure 7 support the conclusion that tris-ligand species participate in the aqueous coordination chemistry of Ti(IV) with citrate in the stated pH range. The data do not distinguish between protonation states because some protonation of the ligand occurs in the instrument under the conditions employed.

In summary, the aqueous solution speciation of titanium(IV) in the presence of excess citrate is revealed by spectropotentiometric titration. In the range pH 3–8, given

the conditions used for the experiments (3-fold molar excess of ligand, 0.1 M ionic strength, 25 °C, argon atmosphere), 3:1 citrate/titanium complexes predominate in solution, and binding of the hydroxide ion is not supported. Log stability constants are determined for these species by least-squares fitting of the potentiometric data, optical spectra are presented, and the X-ray crystal structure for the fully deprotonated $[\text{Ti}(\text{cit})_3]^{8-}$ (**1**) species is reported.

Acknowledgment. Acknowledgment is made to Arthur Tinoco for the synthesis and characterization of the titanium–tris-citrate complex used in several titrations. Acknowledgment is also made to the donors of the Petroleum Research Fund, administered by the American Chemical Society, and to the Research Corporation's Research Innovation Award RI0961, for partial support of this research. This work was also supported with funds from the Yale University Department of Chemistry and through a DuPont Corporation Aid to Education grant.

Note Added in Proof. While this manuscript was in press, a report appeared describing the synthesis and X-ray structures of the complex ion $[\text{Ti}(\text{H}_{0.5}\text{cit})_2(\text{Hcit})]^{6-}$, crystallized from solution at pH 6 (Kefalas, E. T.; Panagiotidis, P.; Raptopoulou, C. P.; Terzis, A.; Mauromoustakos, T.; Salifoglou, A. *Inorg. Chem.* **2005**, *44* (8), 2596–2605). This result is consistent with our speciation, which predicts the predominance of this species (equivalent to $[\text{Ti}(\text{Hcit})_2(\text{cit})]^{6-}$) between pH ~5 and 6.

Supporting Information Available: X-ray crystallographic file of **1** in CIF format, X-ray crystal structure of **1** with sodium counterions and lattice waters included, graphical display of representative fitted titration curves, tabulation of representative least-squares fits of potentiometric data (pdf). This material is available free of charge via the Internet at <http://pubs.acs.org>.

IC048158Y

(54) Huheey, J. E.; Keiter, E. A.; Keiter, R. L. *Inorganic Chemistry: Principles of Structure and Reactivity*; HarperCollins College Publishers: New York, 1993.

(55) Hugi, A. D.; Helm, L.; Merbach, A. E. *Inorg. Chem.* **1987**, *26*, 1763–1768.

(56) Dunand, F. A.; Helm, L.; Merbach, A. E., In *Advances in Inorganic Chemistry*; van Eldik, R., Hubbard, C. D., Eds.; Academic Press: Amsterdam, 2003; p 54.